



Pergamon

DEEP-SEA RESEARCH
PART I

Deep-Sea Research I 45 (1998) 903–930

Chlorofluoromethane distributions in the deep equatorial Atlantic during January–March 1993

Chantal Andrié^{a,*}, Jean-François Ternon^b, Marie-José Messias^a,
Laurent Memery^a, Bernard Boulrès^b

^a*L.O.D.Y.C Laboratoire d'Océanographie Dynamique et de Climatologie,
CNRS/ORSTOM/Université, PARIS, France*

^b*ORSTOM, Institute Français de Recherche pour le Développement en Coopération,
CAYENNE, French, Guiana, France*

Received 7 June 1995, received in revised form 13 December 1996; accepted 20 May 1997

Abstract

Chlorofluoromethanes were sampled along two zonal sections, at 4°30 S and 7°30 N between the African and American continents (A7 and A6 WOCE sections) and two meridional sections, at 35°W and 3°50W, during the CITHER 1 cruise (part of the French program CITHER (Circulation THERmohaline) during January–March 1993. The results reported here deal primarily with the North Atlantic Deep Water, just ten years after the first CFM snapshot of the tropical Atlantic ocean obtained during the Transient Tracers in the Ocean Program (TTO) (Weiss et al., 1985. *Nature* 314, 608–610). The data provide evidence for the eastward bifurcation of the deep flow near the equator, on both UNADW and LNADW levels. The distributions clearly show the CFM signal corresponding to the UNADW penetrating into the eastern basin: at 3°50W the CFM core extends from 4°S to 3°N with a maximum around 2°S. On both UNADW and LNADW levels, the bifurcation does not occur exactly on the equator but a few degrees south and seems to be partly induced by topographic effects. Previously published circulation schemes for UNADW and LNADW levels are compared to the CITHER 1 CFM data. Great variability is revealed and new patterns from the data are highlighted. The “young” deep component of the AABW flow seems to be stopped by the topography just north of the equatorial channel. TTO and CITHER 1 data set comparison and “apparent” ages lead to minimal values of the propagation rate of the CFC signal at low latitudes. © 1998 Elsevier Science Ltd. All rights reserved.

* Corresponding author. Fax: 0033 1 44 27 38 05; e-mail: andrie@lodyc.jussieu.fr



Fonds Documentaire ORSTOM

Cote: B*14807 Ex: 1

1. Introduction

Recently, several authors have discussed the equatorial chlorofluoromethanes distributions (trichlorofluoromethane or CCl_3F or *freon* F-11 and dichlorodifluoromethane or CCl_2F_2 or *freon* F-12, hereafter CFM) inferred from the 1983 TTO data set (Weiss et al., 1985). McCartney (1993) has discussed the issues concerning the Deep Western Boundary Current (DWBC) bifurcation at the equator and the velocity evaluations from tracer distributions. Recirculation processes have been assumed to be partly responsible for the tongue shape of the CFM distributions in the tropical area around 1800 m depth. At this level, the existence of an eastward flow is now well recognized in several circulation patterns (Richardson and Schmitz, 1993; Friedrichs et al., 1994; Rhein et al., 1995). The CITHER 1 data presented here represent a new updated picture of the equatorward spreading of the “young” Upper North Atlantic Deep Water (UNADW) ten years after TTO (Weiss et al., 1985). The enriched CFM core, which classically corresponds to the UNADW, is centered at 1600–1300 m depth and is identified as the recently ventilated shallow NADW, formed by convection in the southern Labrador sea (Fine and Molinari, 1988; Pickart et al., 1989; Pickart, 1992; Molinari et al., 1992; Pickart and Smethie, 1993; Smethie, 1993; Rhein, 1994; Rhein et al., 1995). In addition, the CITHER 1 data describe two other relatively “young” water masses: the Lower North Atlantic Deep Water (LNADW), originating from the Denmark strait overflow (Speer and McCartney, 1991), centered around 3800 m depth and, on the southern section, the Antarctic Bottom Water (AABW).

Several studies (Molinari et al., 1992; McCartney, 1993; Rhein et al., 1995) have suggested that the assumption of an eastward flow from the DWBC at the UNADW level was oversimplified. McCartney (1993) has described two important deep recirculation gyres: the Guiana cyclonic abyssal gyre (in the Demerara plain), centered north of the equator and extending down to 1°S , and the Brazil anticyclonic abyssal gyre (centered at 11°S). Other circulation features have been reported, particularly for the LNADW: Friedrichs et al. (1994) describe a deep equatorial eastward flow, which appears as an important component of the deep circulation (7 Sv flowing eastward compared to the southward DWBC flow of 13 Sv). The existence of a northern abyssal recirculation is also predicted down to the AABW: Kawase (1993) describes through a numerical model a recirculation gyre in the eastern part of the Guiana basin with a northern limit at 25°N .

This paper reports results inferred from CITHER 1 CFM data only. Hydrological and other tracer (oxygen, nutrients) data are described in two companion papers (Ahran et al., in 1998.; Oudot et al., 1998) and in the data reports of Groupe CITHER 1 (1994a–c).

The analytical procedure is presented in Section 2. The main water mass characteristics and circulation features are described and discussed in Section 3. Schematic circulation patterns for the UNADW and LNADW are discussed using the F-11 distributions. In Section 4, we specifically discuss the CFM data as a mean of dating the deep waters. The TTO/CITHER 1 data comparison leads to an estimate of the eastward propagation of the F-11 signal at the UNADW level near the equator. The

“apparent ages” estimated from the F-11/F-12 ratio method give another picture of the tracer field.

2. Data and analytical methods

During the CITHER 1 cruise, January–March 1993, 223 stations were sampled on the R.V. *Atalante* along two zonal sections, at 7°30'N and 4°30' S (A6 and A7 sections of the World Ocean Circulation Experiment WOCE), and on two meridional sections, at 35°W and at 3°50' W (Fig. 1).

Seawater samples were drawn from the IFREMER rosette equipped with 32 8 l bottles: 188 stations were sampled for CFMs on 32 levels regularly spaced from the surface to the bottom, with a spatial resolution around 60 n.m., decreased to less than 30 n.m. near the continental boundaries and close to the equator on meridional sections. Fig. 1 shows the horizontal and vertical sample spacing for the northern section.

The technique used for CFM measurements on board is an extraction-trapping method coupled to gas chromatography with electron capture detection, as described in Bullister and Weiss (1988). Data are reported on the Scripps Institution of Oceanography (SIO) 1986 calibration scale using a primary standard provided by SIO. The accuracy of the secondary standard used on board is 0.9% for F-12 and 0.8% for F-11. The evolution of the primary SIO standard was checked during the WOCE 1991 standard intercomparison experiment (Bullister et al., 1993).

The results of five test-stations for bottle “blanks” determination (32 bottles sampled at the same level, assumed to be CFM free) were used to determine the detection limit of the method. Fig. 2 shows the temporal evolution of the mean contamination

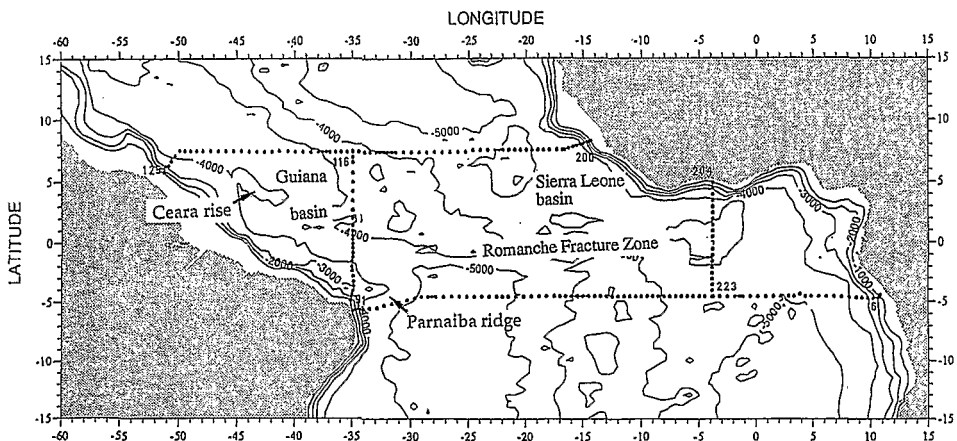


Fig. 1. Station locations of the CITHER 1 cruise in January–March 1993 superimposed on a bathymetric chart showing isobaths at each 1000 m interval. The station numbers corresponding to the end of each leg are indicated.

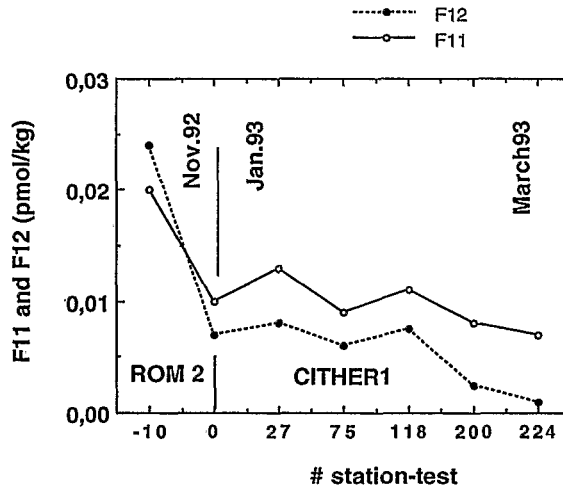


Fig. 2. Evolution of the mean contamination levels (test-stations) measured from November 1992 (Romanche 2 cruise) to March 1993 (CITHER 1 cruise).

level, including 2 test-stations performed during the ROMANCHE 2 cruise (Mercier et al., 1995): the same sampling bottles and the same analytical device were used and left on board the R.V. Atalante between November 1992 and January 1993, in the same laboratory. The mean bottle contamination levels measured by this method vary in the ranges $0.001\text{--}0.008\text{ pmol kg}^{-1}$ for F-12 and $0.007\text{--}0.013\text{ pmol kg}^{-1}$ for F-11. A net decrease of the contamination level occurs after the first week of the ROMANCHE 2 cruise (just one month before the CITHER 1 cruise) which is principally due to progressive *freon* desorption from the PVC bottles (Fig. 2). The final CFM concentrations are corrected for this contamination using two different mean “blank” levels: $0.006\text{ pmol kg}^{-1}$ for F-12 and $0.009\text{ pmol kg}^{-1}$ for F-11 during the first leg of CITHER 1 and $0.002\text{ pmol kg}^{-1}$ and $0.007\text{ pmol kg}^{-1}$ for the second leg. Some very occasional contamination events occurred at a few stations, affecting either F-12 or F-11, due to *freon* adsorption–desorption from o-rings and grease used on two electric plugs above the CTD probe and the rosette motor. These incidents were clearly identified, and the corresponding data (affecting 2 or 3 bottles at fewer than 10 stations) were rejected during the validation procedure. Each individual F-11 and F-12 measured value was validated through the F-11/F-12 ratio (Andrié and Ternon, 1994).

The precision of the method for deep samples is given by the standard deviation of the mean contamination levels: it is around $0.0025\text{ pmol kg}^{-1}$ for F-12 and for F-11. The reproducibility was checked at least once at each station by sampling two bottles at the same depth and is less than 1%. In addition, some stations were reoccupied during the cruise: the deviation between the raw F-11 and F-12 profiles (without blank subtraction) of stations 119–156 at 35°W , $7^{\circ}30\text{ N}$ (15 days apart) is less than 0.5% for F-11 (Fig. 3a). The F-12 measurements are somewhat less reproducible (Fig. 3b),

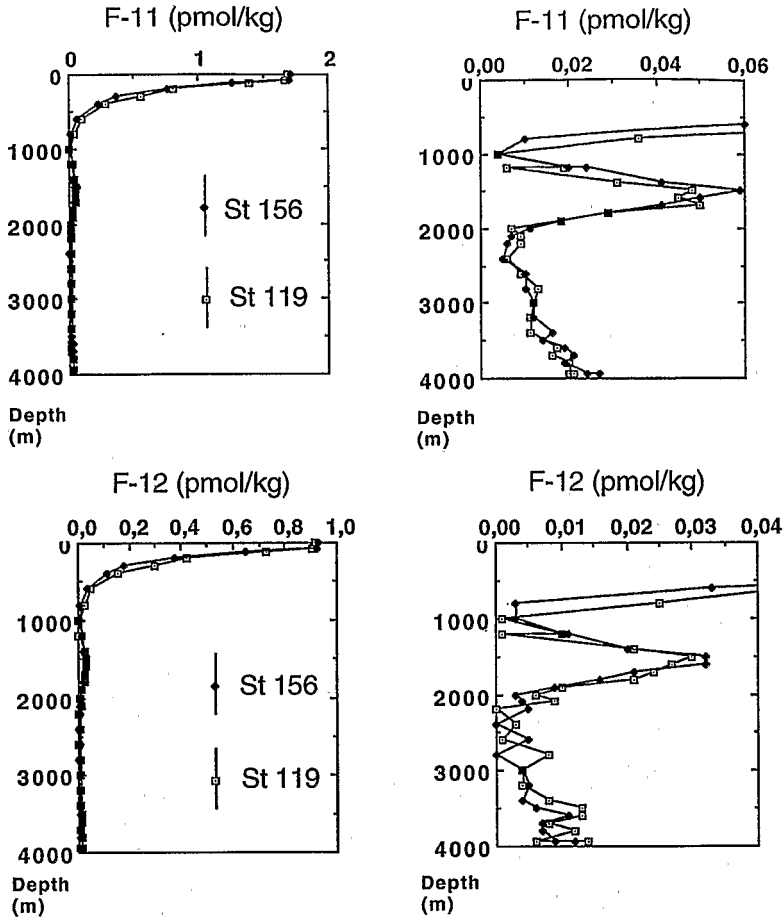


Fig. 3. F-11 and F-12 depth profiles for stations 119 (white squares) and 156 (black squares) samples 15 days apart at 35°W, 7°30' N. (a) For the whole depth range 0–4000 m; (b) for deep waters (F-11 concentrations < 0.06 pmol kg⁻¹).

probably due to the evolution of the blank level between the two legs of the cruise. The deep profiles clearly show the two enriched levels corresponding to the upper and lower NADW, centered at 1600 and 4000 m.

The accuracy of absolute CFM concentrations was checked through atmospheric and surface water distributions.

Atmospheric measurements were performed daily throughout the cruise: a weak latitudinal gradient appears between 7°30' N and 4°30' S (around 0.45 ppt/°lat for F-12 and 0.3 ppt/°lat for F-11); no noticeable zonal gradient was observed, and the mean atmospheric mixing ratios are 513.8 ± 4.2 ppt for F-12 and 276.0 ± 3.2 ppt for F-11 at 7°30' N and 508.3 ± 4.9 ppt for F-12 and 272.4 ± 3.1 ppt for F-11 at 4°30' S (Fig. 4).

We report a mean deviation of the measured surface concentrations to the theoretical solubility values (Warner and Weiss, 1985) close to 1% for both F-12 and F-11

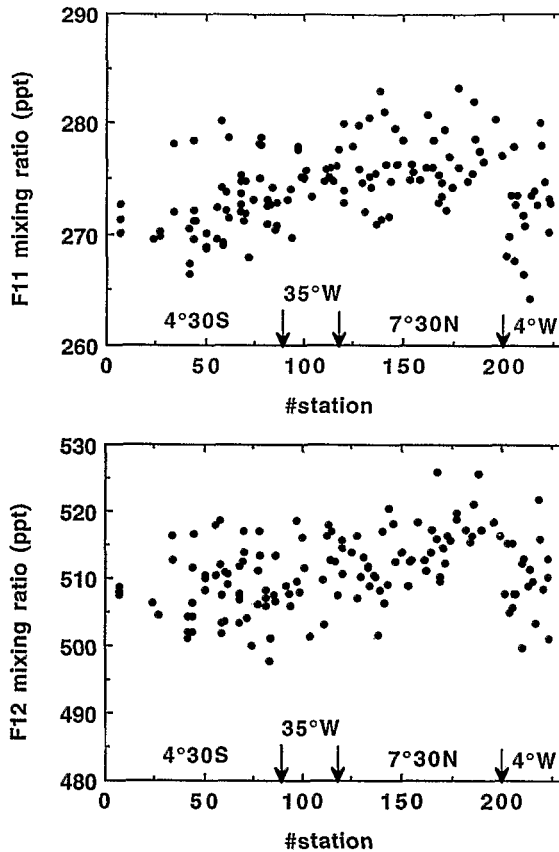


Fig. 4. F-11 (a) and F-12 (b) atmospheric mixing ratios during the cruise.

(Fig. 5a and b): this value, close to the solubility equilibrium, is expected in the tropical area in the northern winter season without strong equatorial upwelling. The low apparent over-saturation is not significant, taking into account the experimental errors (standard concentration, calibration and measurement procedures, etc ...). The values for the stations close to the African continent, off Pointe-Noire-Congo, have been excluded from this global mean (stations 1–15: important undersaturations exceeding sometimes -15% are measured near the coast due to the coastal upwelling (Fig. 5a). The upwelling effect is noticeable on the SST distribution (Fig. 5b).

3. Deep water masses and CFM distributions

The F-11 and F-12 distributions along the $7^{\circ}30'N$, $4^{\circ}30'S$, $35^{\circ}W$ and $3^{\circ}50'W$ sections are shown on Fig. 6. The data set provides original information on the large

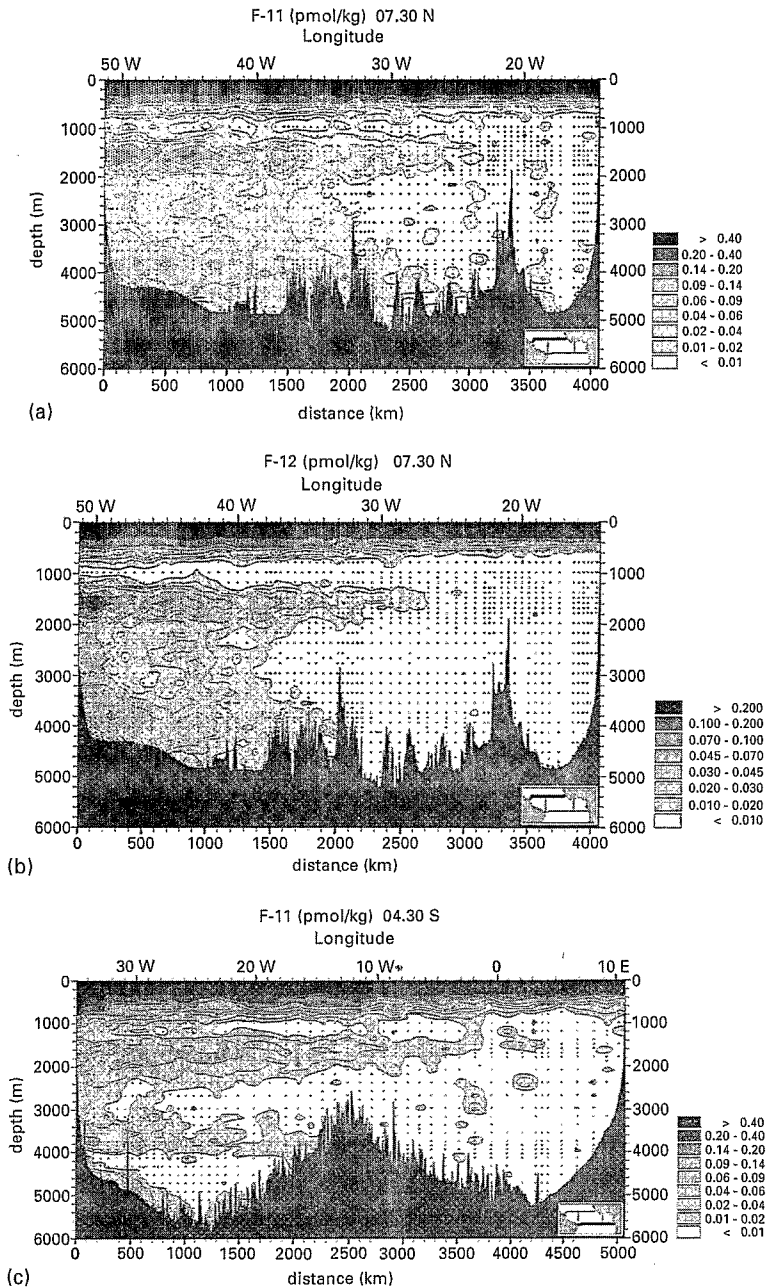


Fig. 6. Vertical CFM distributions during CITHER 1: (a) northern F-11 section (WOCE A6) at 7°30 N (contours in pmol kg^{-1}), (b) northern F-12 section (WOCE A6) at 7°30 N, (c) southern F-11 section (WOCE A7) at 4°30 S, (d) southern F-12 section (WOCE A7) at 4°30 S, (e) meridional western F-11 section at 35°W, (f) meridional western F-12 section at 35°W, (g) meridional eastern F-11 section at 3°50W and (h) meridional eastern F-12 section at 3°50W.

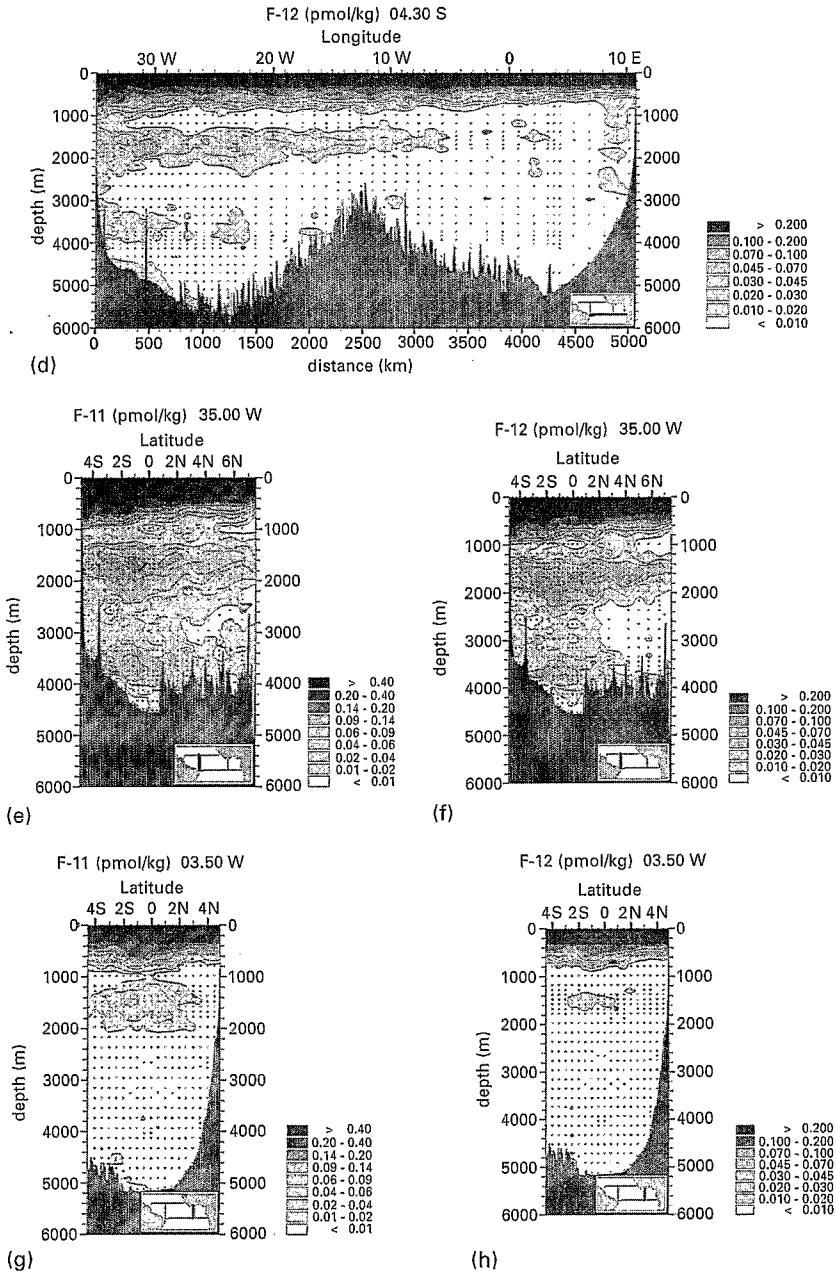


Fig. 6. (continued).

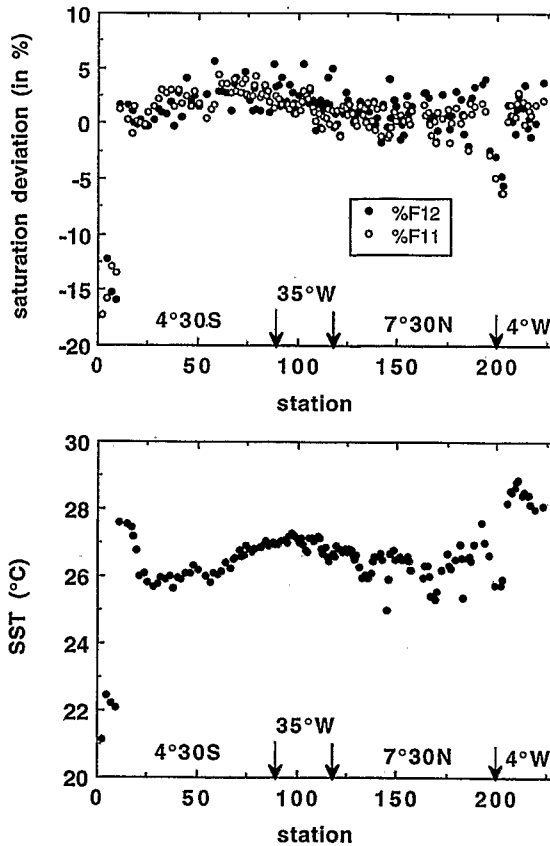


Fig. 5. (a) Saturation anomaly for F-11 (white squares) and F-12 (black squares) as a function of station number (saturation deviations from the theoretical atmosphere equilibrium value are derived from Warner and Weiss, 1985). (b) Sea surface temperature SST during the cruise.

scale transient tracer distribution in this area with an adapted vertical and horizontal sampling resolution, which was particularly narrow at the UNADW and LNADW levels.

A striking feature inferred from these distributions is the large spatial variability observed in the CFM concentrations. The significance of this small scale variability is insured by the similarity of both F-11 and F-12 distributions (compare Fig. 6a and b; c and d; e and f; g and h) and by the value of the observed gradients ($0.01 \text{ pmol kg}^{-1}$ between deep adjacent isolines), well above the detection limit of the analytical method.

In order to describe and discuss the principal circulation features of the deep western tropical Atlantic we refer in the following to the circulation patterns proposed by Friedrichs and Hall (1993) – hereafter F&H93 – and Friedrichs et al. (1994) – hereafter F&al.94 – from geostrophic calculations and property distributions, for three

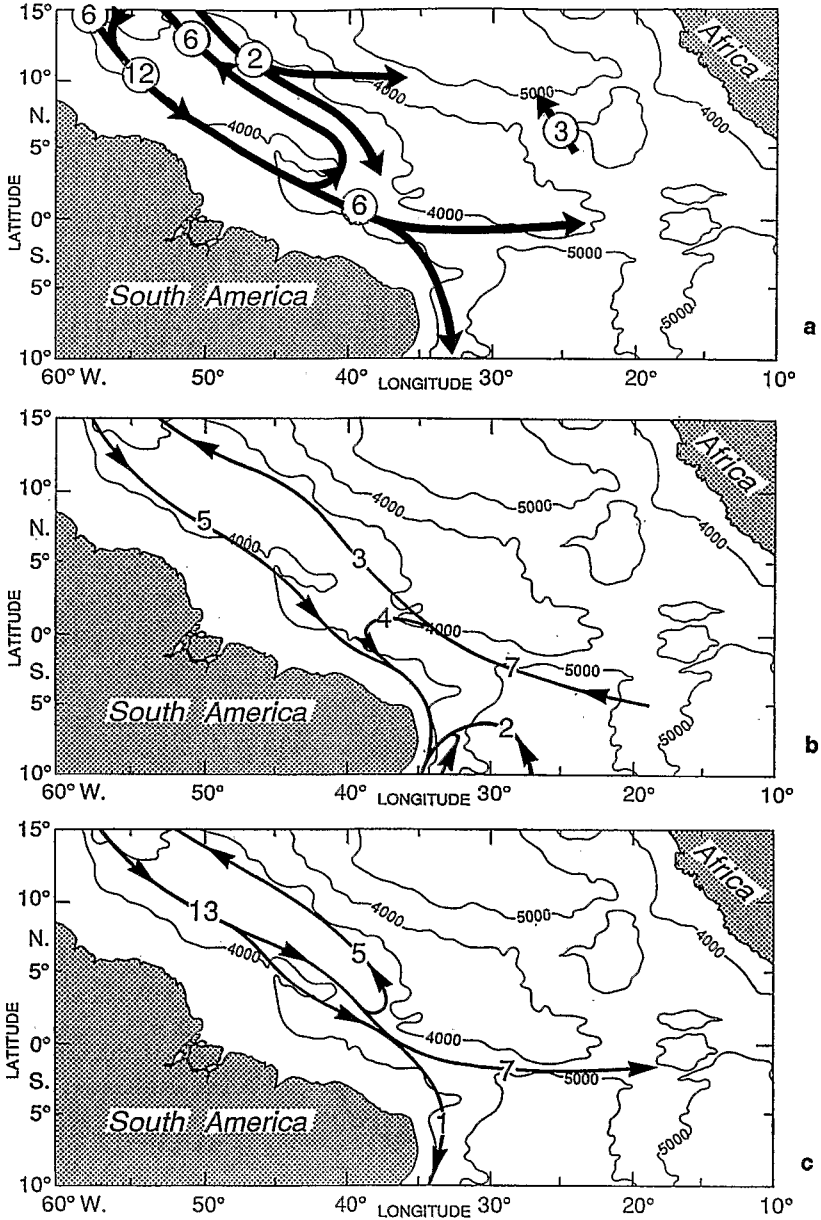


Fig. 7. General circulation patterns inferred from previously reported hydrological data and transport calculations: (a) UNADW level, from Friedrichs and Hall (1993) (in the text F&H93); (b) MNADW level, from Friedrichs et al. (1994) (in the text F&al.94); (c) LNADW level, from Friedrichs et al. (1994) in the text F&al.94.

particular NADW levels (Fig. 7a–c): upper NADW, middle NADW and lower NADW. We successively discuss CFM distributions for depths below the Antarctic Intermediate Water (AAIW) level (800–1000 m depth) down to the bottom.

3.1. Upper circumpolar water

An almost totally *freon*-free water mass is a particular feature of the Atlantic ocean in the range 1000–1200 m (Figs. 3 and 6). This level was described by Kawase and Sarmiento (1986) as a poorly ventilated (low oxygen concentration) and nutrient rich level. The absence of CFMs at this depth, in the northern section as well as in the southern one, characterizes the “old” Upper Circumpolar Water (UCPW) coming from the south, without any ventilation at southern latitudes (Reid, 1994). Unlike previous observations (Fine and Molinari, 1988; F&H93; Tsuchiya et al., 1994; Bub and Brown, 1996), the UCPW is unambiguously identified through the very low CFM contents measured during CITHER 1, distinct from the ventilated *freon*-rich AAIW: The AAIW salinity minimum is located around 800 m (Groupe CITHER 1, 1994b; Arhan et al., 1998) associated with F-11 concentrations significantly higher than at 1000 m depth. The 1000 m in UCPW level corresponds to a silicate maximum (Oudot et al., 1998). The F-11 minimum layer is around 200 m deeper at 4°30S than at 7°30N (1200 m versus 1000 m; Fig. 6a and c) as the result of the erosion of the minimum by the CFM-rich UNADW in the north.

3.2. Upper North Atlantic deep water

The maximum observed in the F-11 distribution centered in the depth range 1600–1700 m (Fig. 3) corresponds to the “shallow” UNADW (or SUNADW after Rhein et al., 1995), hereafter referred as UNADW. It originates from the southern Labrador Sea Water (Pickart et al., 1989; Smethie, 1993) and feeds the upper part of the DWBC. Previous upstream observations in the DWBC (Molinari et al., 1992; Rhein et al., 1995) have shown that the F-11 cores coincide with southward velocity cores.

Fig. 7a (F&H93) describes the principal circulation features of the UNADW:

- a mean southward flow within the DWBC, which partly bifurcates eastward near the equator and partly continues southward across the equator along the American shelf.
- a large recirculation cell, the deep Guiana gyre, corresponding to a strong southward flow trapped against the western boundary and, offshore, a northward flow representing the recirculating component of the DWBC (Molinari et al., 1992; McCartney, 1993). The northward limb of the gyre is supposed to be narrow and located directly over the deepest part of the Guiana basin.
- a southward flow is located over the western flank of the Mid Atlantic Ridge (MAR). This flow is assumed by F&H93 to continue south of 11°N. Its possible eastward extension either over the MAR or near the equator is still questionable.

The 7°30N section (Fig. 6a and b) is very similar to the one obtained by Molinari et al. (1992) during February 1989 along a zonal transect at 14°30N. The F-11 enriched core located around 50°W, close to the American continent, is due to the DWBC itself. The F-11 maximum ($> 0.32 \text{ pmol kg}^{-1}$) is associated with a salinity maximum (> 35.01) and a silicate minimum ($< 15.2 \text{ } \mu\text{mol kg}^{-1}$; Groupe CITHER 1, 1994c). The width of the tracer core is somewhat extended offshore (compared to the DWBC velocity core); this is due to the turbulent mixing occurring between DWBC and the southward western branch of the cyclonic Guiana recirculation gyre. Around 45°W, a second F-11 maximum core ($> 0.22 \text{ pmol kg}^{-1}$) reflects the presence of the eastern limb of the recirculation gyre. It is associated with a salinity maximum (> 35.00) and a silicate minimum ($< 16.0 \text{ } \mu\text{mol kg}^{-1}$). The northward flow extends offshore to 41°W. Between the two cores, the low F-11 concentration (around 47°W) corresponds to the less energetic central area of the recirculation cell.

A third CFM maximum is noticeable farther east, around 38°W. This core coincides with a salinity maximum and silicate minimum (Groupe CITHER 1, 1994b, c), and therefore seems to be a permanent feature of the circulation. This CFM maximum seems to correspond to a particular structure in the CITHER 1 density distribution at 1600–1800 m (Fig. 4, Arhan et al., 1998) and could be associated with the southeastward flow as suggested by F&H93 (Fig. 7a). Nevertheless, from the available data, we cannot determine the origin of this saline and *freon*-rich water mass. Other mechanisms can be responsible for the tracer maximum at 38°W. We cannot exclude the effect of nonpermanent northward flow, fed by the recirculation gyre, or a second cyclonic deep circulation cell as previously described in the eastern basin (McCartney et al., 1991; McCartney, 1993; F&H93; F&al.94). Such a discontinuity in the upper core can also be attributed to disruptions in the zonal advective flow or in the deep water mass formation rates in the last 20 years (Fine and Molinari, 1988; Dickson et al., 1990; Doney and Jenkins, 1994; Dickson and Brown, 1994; Weisse et al., 1994). To the west of this structure, around 40°W, the CFM minimum could correspond to a no-motion area (Fig. 7a) or to southern waters coming from the east.

On the 35°W section (Fig. 6e) we observe three main low F-11 concentration areas: near the South American boundary, around the equator and around 3–4°N. In between, two F-11 concentration maxima are identified south and north of the equator. A third maximum is located around 5°N.

The first maximum area, between 1 and 3°S (maximum F-11 concentration $> 0.11 \text{ pmol kg}^{-1}$), was observed in October 1990 and June 1991 by Rhein et al. (1995); during CITHER 1, it is undoubtedly linked to a well established eastward flow on the corresponding Pegasus profile (Colin et al., 1994a). It is associated with low silicate and high salinity values ($< 17.5 \text{ } \mu\text{mol kg}^{-1}$ and > 34.985 ; Groupe CITHER 1, 1994c). According to the F&H93 representation (Fig. 7a), this core is fed, around 3°S, by the DWBC itself, after its crossing of the equator. Around 1°S, the core corresponds to the eastward bifurcated flow. The depth of the F-11 core is shallower (1500–1600 m; Fig. 6e) at 3°S than at 1°S, reflecting a lower input of the northward low-*freon* counterflow into the upper part of the UNADW.

Around 2°N, a second F-11 core is observed (maximal F-11 concentration $> 0.11 \text{ pmol kg}^{-1}$). It was previously observed during October 1990 and June 1991

(Rhein et al., 1995). The direction of the associated flow does not seem to be permanent: Rhein et al. (1995) describe alternate westward and eastward velocities; three equatorial float trajectories between January 1989 and September 1992 (Richardson et al., 1994) do not describe any permanent flow around 2°N. During CITHER 1, the comparable CFM concentrations at 2°N and at 3°S ($> 0.1 \text{ pmol kg}^{-1}$) suggest that the F-11 core at 2°N is fed directly from the DWBC by an eastward flow. Silicate and salinity data also support this assumption (Groupe CITHER 1, 1994b, 1994c). This flow can be part of the Guiana gyre's southern closure, north of the equator. Unfortunately, there is no direct current measurement at the time of the CITHER 1 cruise at 2°N.

A northward extension of a F-11 core as far as 6°N is shown on the 35°W section (Fig. 6e). This feature seems to be directly linked to the CFM core observed around 38°W on the 7°30' N section, presumably associated with a southeastward flow. F-11 concentrations decrease from 0.1 pmol kg^{-1} at 7°30' N, 38°W (Fig. 6a) to $0.065 \text{ pmol kg}^{-1}$ at 5°N, 35°W (Fig. 6e), in agreement with this assumption. The silicate distribution (Oudot et al., 1998) shows a minimum at the location of the CFM core, with indications of a decreasing northern influence from 7°30' N, 38°W ($15.8 \text{ } \mu\text{mol kg}^{-1}$) to 5°N, 35°W ($17.5 \text{ } \mu\text{mol kg}^{-1}$).

On both northern and southern CITHER 1 CFM sections, the centers of the recirculation gyres are located around 450 km off the American continent (F-11 minima around 47°W at 7°30' N, 35°W at the equator, 31°W at 4°30' S). The CFM recirculating branch appears broader than in the F&H93 pattern on Fig. 7a. The other circulation features inferred from the CFM distribution correspond well to the F&H93 pattern (Fig. 7a). The location of the southern closure of the recirculation is not obvious from the 7°30' N and 4°30' S zonal sections (Fig. 6a and c) alone. The F-11 horizontal distribution at the UNADW level is more contrasted in the north than in the south, with an important recirculated core located 700 km offshore (45°W on the 7°30' N section). Such a core is not so distinctly observed on the 4°30' S section, which can result from the very low F-11 levels or which could indicate that the recirculation closure should take place north of 4°30' S.

One of the most important features of the CITHER 1 CFM distributions is the CFM core (centered around 2°S) observed along the 3°50'W section in the eastern basin, around 1500–1600 m (Fig. 6a and h). The hydrological characteristics of the CFM cores observed around 1600 m indicate the continuity between the two cores (at 35°W station 101, $F-11_{\text{max}} = 0.109 \text{ pmol kg}^{-1}$, $\sigma_{\theta} = 27.767$, $S = 34.985$; at 3°50'W station 217, $F-11_{\text{max}} = 0.041 \text{ pmol kg}^{-1}$, $\sigma_{\theta} = 27.783$, $S = 34.977$ at 3°50' W). The F-11 input observed as far east as 4°W is clearly linked to the zonal bifurcation of the deep flow. The F-11 tongue results from the splitting of the DWBC at low latitudes in an eastward flow and a continued southward flow.

The data support the earlier interpretation of Weiss et al. (1985) and Doney and Bullister (1992) for the existence of an eastward flow coming from the bifurcation of the DWBC near the equator. The "along-equator" component of the DWBC is not located just at the equator, but the core maximum is somewhat shifted south of the equator (around 2°S). This is in agreement with Tsuchiya et al. (1992, 1994), who report from two salinity sections an eastward core centered around 2°S at 25°W.

Durrieu de Madron and Weatherly (1994) refer also to an eastward extension of the NADW flow, but they locate the DWBC bifurcation, responsible for the significant flow decrease in the southern basin, around 5°S.

The bifurcation could partly be due to dynamic effects induced by the topography of the Parnaíba ridge near 3°S (rise around 2000 m depth, see Fig. 1) and by the DWBC forcing itself (Kawase, 1987). On the other hand, Hua et al. (1997) explain the generation of deep equatorial jets by inertial nonlinear equilibration. They describe a resulting meridional shift of the zonal jets a few degrees from the geographic equator, which corresponds to the CFM core location.

Continuity of the DWBC and its connection to zonal flow near the equator have been emphasized through the trajectories of floats launched in the DWBC at 1800 m depth (Richardson et al., 1994). Eastward trajectories along the equator show established flows for several years, but they are not permanent, alternating with a southward DWBC crossing the equator.

Features inferred from the tropical CFM distribution (presence of a *freon* core at 4°W, shift of the equatorial signal south of the equator, etc ...) must be considered as very strong constraints on equatorial circulation modelling to understand and quantify the eastward flow.

3.3. Middle North Atlantic deep water

The layer 1900–3400 m corresponds to the Middle NADW (MNADW), after F&H93. This denomination includes the Labrador Sea Water (LSW), the Gibbs Fracture Zone Water (GFZW) from the north and a southern Circumpolar Water (CPW) component (Reid, 1994; Rhein et al., 1995). These water masses have relatively low CFM contents (Fig. 3), for different reasons: oxygen content in LSW is high due to convection and weak oxygen consumption, but incomplete convection occurring during the 1960s and 1970s is responsible for the weakness of the transient tracer concentrations (Lazier, 1973, 1988; Talley and McCartney, 1982; Wallace and Lazier, 1988; Dickson et al., 1990). The different boundary conditions, long transit time and mixing undergone by the GFZW are responsible for its oxygen, tritium and CFM minima compared to the CFM-rich layers corresponding to the UNADW and the LNADW (Doney and Jenkins, 1994; Rhein et al., 1995).

Fig. 7b reports the circulation pattern proposed from geostrophic calculations by F&al.94 for the MNADW level. They describe a southward flow inside the DWBC and a northward flow along the western flank of the MAR assumed to be from a southern origin, with a possible connection between both opposite branches. From the F&H93 (not reported here) and F&al.94 patterns, as well as from the 3300 m float trajectories (Richardson and Schmitz, 1993), there is no evidence for an eastern equatorial flow.

Expected on the western boundary (Fig. 6), CITHER 1 CFM concentrations are low in this depth range. Nevertheless, we observe, along the 7°30' N section, relatively high CFM concentrations inside the DWBC, from the continent to 300 km offshore. Such concentrations from 2000 m down to 3500 m depth, can be the result of mixing between UNADW and LNADW during their displacement from the north inside the

DWBC. The signal could also be attributed to an increased input of LSW or GFZW since the 1990s. The assumed shut-off of deep convection in LSW during the late 1960s could have been the reason for the absence of a CFM signal in this depth range in previous works (Molinari et al., 1992; Rhein et al., 1995).

A dramatic feature on the 7°30 N section (Fig. 6a and b) is the presence of a relatively CFM enriched water mass around 42–45°W, which seems to be continuous from the UNADW to the LNADW level, including the MNADW, as observed inside the DWBC itself. The F&H93 pattern at the MNADW level (Fig. 7b) does not clearly indicate the feeding of this CFM core offshore by the northwestward limb of the Guiana gyre. Our data, on the other hand, give evidence for a continuous recirculated northward flow in the whole deep water column including, particularly, the 2200–3000 m depth range.

In contrast with the CFM enriched waters, the existence of *freon-free* waters can correspond, in the center of the recirculation, to the tracer minimum described through an advective-diffusive model by Pickart and Hog (1989): as for the UNADW level, the *freon-free* core observed between 2000 m and 3200 m on the 7°30 N section, is centered at 450–500 km off the American continent, in the center of the deep cyclonic Guiana gyre. On the other hand, some *freon-free* CPW coming from the South is assumed to interfere with northern water and to contrast with the recirculated flow (Reid, 1994; Tsuchiya et al., 1994; Talley and Johnson, 1994; F&al.94; Rhein et al., 1995). On the 35°W section, around 3000 m depth, there are two *freon-free* structures at 2°S and near the equator (Fig. 6e). These cores are associated with a low salinity and a silicate enrichment (respectively < 34.93 and $> 33 \mu\text{mol kg}^{-1}$; Groupe CITHER 1, 1994c) and so can be attributed to southern water input (Speer, 1993). Other *freon-free* structures are observed on the southern 4°30S section (Fig. 6c) around 3000 m, 450 km and 1000 km offshore, less saline and with a higher silicate content than those observed at 35°W (respectively < 34.925 and $> 34 \mu\text{mol kg}^{-1}$). They are similar to the “cat-eye” structures described by McCartney (1993) and can correspond to a CPW component flowing northward along the western side of the MAR as described by F&al.94 (Fig. 7b).

The southern water input does seem dominant through the CITHER 1 F-11 distribution on the 7°30 N section, where a deep recirculation cell on the whole water column is described. This suggests a north-south asymmetry of the circulation at the MNADW level, similar to the recirculation pattern observed at the UNADW and LNADW levels (Fig. 7a and c). For the MNADW level, the CFM CITHER 1 data does not agree with the F&al.94 circulation pattern (Fig. 7b).

3.4. Lower North Atlantic deep water

The F-11 maximum centered at 3800–4000 m depth corresponds to the “overflow” LNADW (OLNADW after Rhein et al., 1995), mostly originating from the Denmark strait overflow (Pickart et al., 1989; Smethie, 1993). Fig. 7c gives the F&al.94 circulation pattern for the LNADW level. They describe, as discussed for the UNADW level, a strong southward flow within the DWBC. A recirculation cell exists, assumed to occur north of the equator. Less than 10% of the flow is supposed to be transported

southward across the equator and, to explain this transport asymmetry, the authors argue for an eastward bifurcation along the equator in addition to the recirculation gyre. The eastward flow partly feeds an upwelling between LNADW and MNADW in the eastern basin. One explanation for the F&al94 MNADW pattern (Fig. 7b) is that the flow of LNADW passing into the eastern basin through the Romanche Fracture Zone (RFZ) is volumetrically compensated for by a westward flow of warmer water at the MNADW level.

The distribution along the 7°30 N section (Fig. 6a) clearly shows the recirculating branch of the Guiana gyre around 42°W, somewhat offshore compared to the UNADW and MNADW levels due to the topography.

At 7°30 N, in the western part of the Guiana basin, from the continent to 40°W, the main structure of the LNADW cores is very similar to that of the UNADW, principally due to the recirculation gyre (McCartney, 1993; F&H93). The large and homogeneous concentrations observed at 7°30 N, between the continent and 40°W (Fig. 6a and b), are the results of the blocking of the LNADW by the Ceara rise, the water flowing eastward along the topography (see the 4000 m isobath on Fig. 1).

South of the Ceara rise, the deep flow turns southward again, stuck against the continental slope. Near the equator, the deep flow is blocked by the Parnaiba ridge and is partly diverted eastward along the equatorial channel (see Fig. 7c; F&al.94; Molinari et al., 1992; Rhein et al., 1995).

A striking feature of the CITHER 1 distributions is that, on the western boundary (Fig. 6a and c), the F-11 maximum reaches $0.14 \text{ pmol kg}^{-1}$ at 7°30 N when it is only $0.04 \text{ pmol kg}^{-1}$ at 4°30 S (for comparison, hydrological characteristics at 3800 m are respectively $\sigma_\theta = 27.897$, $S = 34.897$ at 7°30 N and $\sigma_\theta = 27.889$, $S = 34.903$ at 4°30 S). This north-south asymmetry is more pronounced than at the UNADW level. This particular LNADW asymmetry is also observed on salinity sections (Arhan et al., 1998) and does not seem linked to the transient behavior of CFMs. This is partly the result of the eastward bifurcation of the LNADW near the equator, as previously suggested by F&al.94 and Rhein et al. (1995).

At 35°W (Fig. 6e) the F-11 core is centered at 1°40 S within the equatorial channel between the Parnaiba ridge at 2°S and the equator (see the 4000 m isobath on Fig. 1); the core seems to follow the southern flank of the equatorial channel, the northern flank preventing the northward extension of the flow. It corresponds to a permanent eastward narrow jet around 1°30S, at 3900 m, as evidenced through the equatorial channel from mooring records at 35°W between October 1992 and June 1994 (Hall et al., 1997). It has already been mentioned by Rhein et al. (1995) through CFM data and direct velocity measurements (Pegasus and L-ADCP). Another part of the deep flow continues southward along the South American continent (Fig. 6c): south of the equator, the southward flow at 3800 m is less CFM enriched, warmer, more saline and less oxygenated than the eastward flow inside the equatorial channel (Groupe CITHER 1, 1994b, c), perhaps as the signature of mixing with MNADW.

The CFM signal found in the RFZ at the LNADW level (Messias et al., 1998) is the unquestionable signature of the eastward flow along the equator. The F-11 signal observed at 3°50W during CITHER 1 in the depth range 4500–5000 m (Fig. 6g) is likely to be the continuation of the eastward deep flow along the RFZ (for comparison

$\sigma_\theta = 27.890$ at 3800 m, station 100 along 35°W and $\sigma_\theta = 27.880$ from 3800 m to the bottom, station 216 along $3^\circ50\text{W}$). The F-11 signal results from the intense mixing between LNADW and AABW below 4000 m (Polzin et al., 1996) and their cascading and spreading from the sills of the RFZ (Mercier et al., 1994; Mercier and Morin, 1997; Messias et al., 1998). Another F-11 enriched cell observed on the $7^\circ30\text{N}$ section (Fig. 6a) could originate from a deep component flowing out of the RFZ inside the Sierra Leone basin.

At the LNADW level, the CFM CITHER 1 data set emphasizes the eastward bifurcation of the deep flow and the existence of the recirculation abyssal Guiana gyre as depicted through the F&al.94 circulation pattern (Fig. 7c).

3.5. Antarctic bottom water

The southern $4^\circ30\text{S}$ section (Fig. 6c and d) exhibits a CFM enriched core, lying on the bottom below 4500 m, corresponding to an AABW component. This core is noticeable on the western side of the Brazil basin, near the South American continent. As mentioned by Rhein et al. (1995), this water mass is CFC enriched by mixing with the more recently ventilated underlying Weddell Sea Bottom Water (WSBW). Tsuchiya et al. (1994) make a more precise distinction between an “older” component of the AABW, of Lower Circumpolar Water origin, and a “newer” one, the WSBW.

Inside the Brazil basin, our data clearly suggest that the “newer” component of the AABW is located only on the western side of the Brazil basin, identified by a freon core. An “older” component lies on the eastern side of the basin, corresponding to freon-free water (Fig. 6c). The slightly CFM enriched bottom water around 26°W at $4^\circ30\text{S}$ (Fig. 6c) could be the result of a recirculating southward AABW flow as suggested by Durrieu de Madron and Weatherly (1994).

On the 35°W section, the freon-free core observed in the southern part of the channel (Fig. 6e, around $1^\circ30\text{S}$) probably corresponds to a permanent westward flow observed in this area. LADCP measurements from 1990 to 1992 (Rhein et al., 1995), velocity records from moorings (Hall et al., 1997; Fischer and Schott, 1997) and Pegasus profiles at the time of the CITHER 1 cruise (Colin et al., 1994a) show that a mean westward bottom current is principally present south of the equator at the same location as the LNADW maximum corresponding to the eastward flow around 3800 m (near $1^\circ30\text{S}$). The AABW corresponding to the velocity core, associated with a CFM minimum, seems to have a predominant LCPW component. There was no evolution of the bottom F-11 concentration at $1^\circ30\text{S}$, 35°W from the 1990–1992 data (Rhein et al., 1995) to 1993; this confirms that the AABW westward flow in the south of the equatorial channel is principally a LCPW component (Rhein et al., 1995). Nevertheless, in the deepest part of the channel (latitude $0^\circ39\text{N}$, about 4550 m depth) we observe, just above the bottom, high F-11 and silicate concentrations and low potential temperature ($> 0.016\text{ pmol kg}^{-1}$, $> 109\text{ }\mu\text{mol kg}^{-1}$ and $< 0.56^\circ\text{C}$; Groupe CITHER 1, 1994b), which reflect the presence of WSBW component.

On the $7^\circ30\text{N}$ section (Fig. 6a and b) there is no CFM signal. McCartney and Curry (1993) suggest two reasons for restriction of the northward flow of AABW: the sill at the entrance of the equatorial channel and then the Ceara rise acting as a barrier

1°N and 4°N. As observed on the 35°W section, the topographic effects block a northward passage for the “younger” lower WSBW component. The upper component, *freon-free* LCPW, is identified through silicate data ($> 74 \mu\text{mol kg}^{-1}$ at 7°30 N/40°W, above the bottom; Groupe CITHER 1, 1994c).

As mentioned above, we attribute the F-11 signal observed at the bottom of the eastern basin (Fig. 6g) to the deep flow from the Romanche fracture zone (Mercier and Morin, 1997; Messias et al., 1998), mixing of LNADW and AABW. The weakness of the F-11 signal is linked to the topographic effects, west of the MAR, which block any direct input of “young” WSBW component.

4. “Apparent” ages and velocities

The “apparent” ages and dilution factors were estimated for the UNADW using the atmospheric mixing ratio time evolution for the northern hemisphere and the solubility functions for F-11 and F-12 from Warner and Weiss (1985). In Fig. 8 are reported the derived time evolutions of the UNADW-F-11 content and the corresponding F-11/F-12 ratio. Theoretical F-11 (and F-12) concentrations are calculated assuming no dilution since the CFM dissolution at the ocean-atmosphere interface and considering the temperature and salinity of the UNADW during CITHER 1. The “age” is computed from the time evolution of the theoretical UNADW F-11/F-12 ratio (11/12 curve on Fig. 8). The inferred “apparent” velocity is the distance between the sampled area and the formation area (southern Labrador Sea for the UNADW) divided by the measured F-11/F-12 age of the water parcel. The dilution factor is

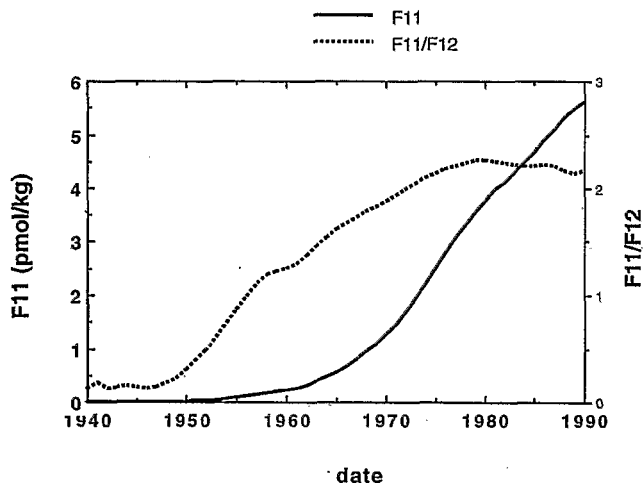


Fig. 8. Temporal evolution of the theoretical oceanic F-11 concentration (solubility equilibrium) and the corresponding F-11/F-12 ratio evaluated from the time history of the atmospheric F-11 concentrations. The temperature and salinity used in the solubility function of Warner and Weiss (1985) are relative to the UNADW.

defined as the theoretical F-11 content at the time of the UNADW formation (F-11 curve on Fig. 8) divided by the measured F-11 concentration at the time of the sampling.

A limitation for the “apparent age” at low latitude, away from the deep CFC sources, is that the “age” applies only to the fraction of the DWBC water parcel that has left the surface before being diluted.

In our UNADW age calculations, no correction has been made for the CFM undersaturation in the formation area (Wallace and Lazier, 1988), nor for the time spent by the newly convected water in reservoirs feeding the DWBC (Pickart et al., 1989), nor for mixing. Recent relevant transient tracer distribution studies have shown difficulties in data analysis inherent to turbulent mixing processes occurring between the mean flow and the surrounding waters, and responsible for a bias in apparent age or velocity determination (Pickart, 1992; Smethie, 1993; McCartney, 1993; Rhein, 1994; Doney and Jenkins, 1994). Self-mixing and recirculation are known to lead to older tracer ages and slower estimated velocities, and consequently the reported evaluations cannot represent actual age, velocity or dilution factor. Nevertheless, Doney and Jenkins (1994) argue that “transient trace velocities, although poor indicators of the velocity of the boundary current itself due to mixing, may be a good estimate of the net effect of mixing and recirculation effects over the length of the boundary current system”. They compare the transient tracer apparent velocity to a “spreading rate”, which gives an overall integral aspect of the system. Both quantities result from the combined effects of along-stream advection and cross-stream mixing and recirculation over the length of the boundary current system.

The distributions of the “apparent ages” calculated from the F-11/F-12 ratio method on each section of the CITHER 1 cruise are shown on Fig. 9a–d. In such distributions the significant “age” values range from about 20 to 40 years. After 1975 (for ages smaller than 20 years), the F-11/F-12 became constant, and consequently the method can give only an upper bound of the age estimate. On the other hand, the F-11/F-12 ratios calculated for F-11 concentrations lower than $0.01 \text{ pmol kg}^{-1}$ lead to very inaccurate “age” estimate (more than 100% error): this corresponds approximately to “ages” greater than 35–40 yr.

The principal features inferred from the F-11 and F-12 distributions (Fig. 6) are supported by the “age” distributions (Fig. 9). The two tongues of “young” waters corresponding to the UNADW and LNADW levels and the imprint of the “old” UCPW around 1000 m depth are noticeable. The youngest waters (“age” around 20 years) are principally observed along the northern section ($7^{\circ}30 \text{ N}$). Young waters are observed as far east as $3^{\circ}50 \text{ W}$ (near the equator, Fig. 9). “Old” patches (> 35 years) are located in areas of relative no-motion waters and allow specification of the location of the recirculation cell centers associated with low advection velocity and low mixing: on the 35° W section in the range 2600–3000 m, between the equator and 1° N , and around 3° S ; on the $7^{\circ}30 \text{ N}$ section, around 3000 m near 40° W , and around 48° W at 2200 m.

In the western $7^{\circ}30 \text{ N}$ section, the “age” distribution is quite homogeneous. This feature is undoubtedly due to the stable level of the F-11/F-12 ratio after 1975, the ratio reaching its upper limit (2–2.1) in this area (Fig. 8). For this reason, the “age”

structure observed in the east of the western basin cannot be interpreted as a continuous evolution of the western structures. Also, because of the constancy of the F-11/F-12 ratio for “young” waters, no sharp difference appear between UNADW, LNADW and AABW.

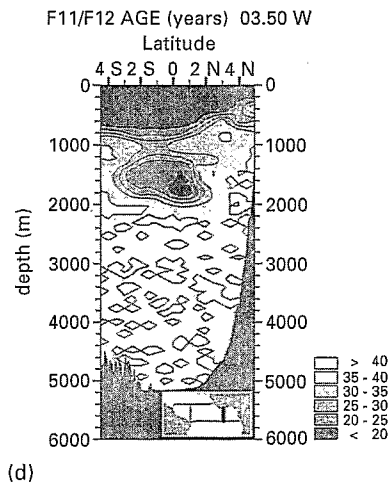
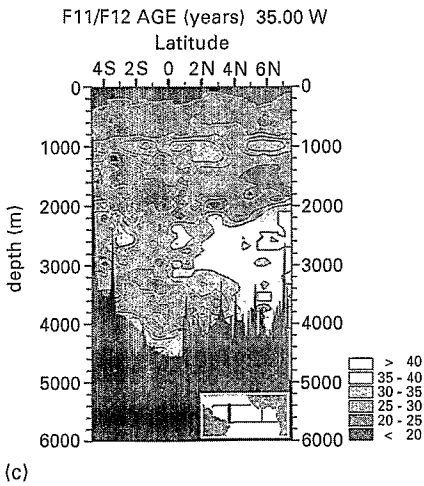
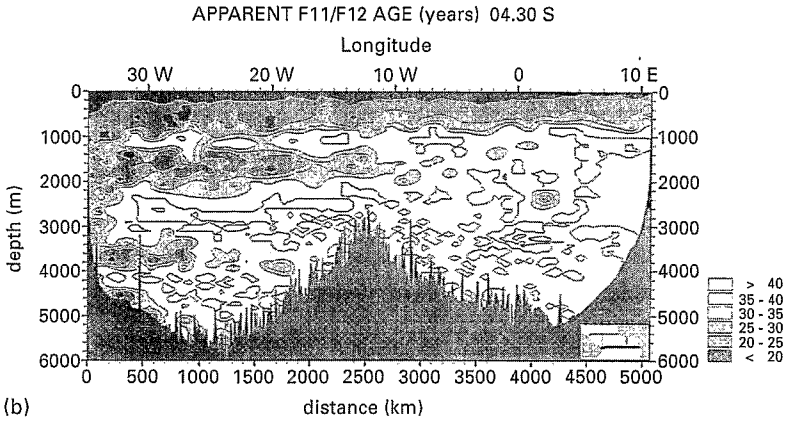
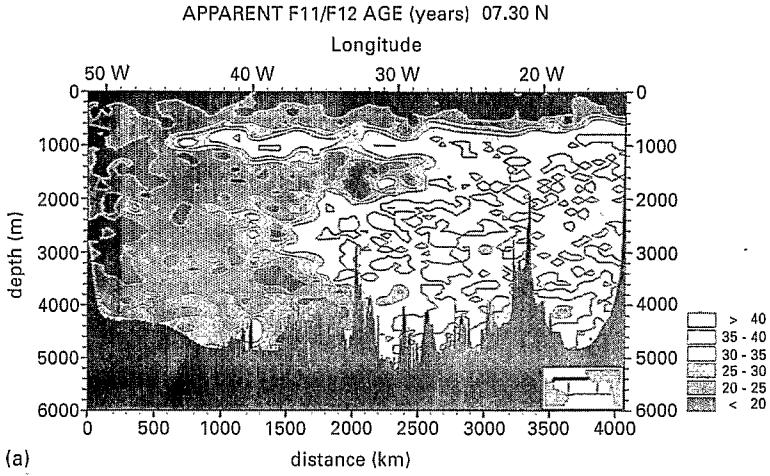
The limitations of the F-11/F-12 method are particularly evident in the west. The relative constancy of the apparent velocity ($1.6\text{--}1.9\text{ cm s}^{-1}$) estimated in the west is linked to the age homogeneity within the DWBC (Fig. 9a). Nevertheless, it can be compared to the tracer-derived velocity (from tritium/helium-3 age, $0.75\text{--}1.5\text{ cm s}^{-1}$) estimated by Doney and Jenkins (1994) for the DWBC. They consider this evaluation very similar to the “spreading rate” for newly formed NADW in the western basin, taking into account turbulent mixing and recirculation processes occurring between the mean flow and the surrounding waters. The “apparent” velocity field and the real physical advection field are two completely different concepts. The flow speed measured by direct observations is considerably higher than the apparent speed obtained by the F-11/F-12 method: Colin and Bourlès (1994) and Colin et al. (1994b) report Pegasus and currentmeter velocity measurements greater than 50 cm s^{-1} in the area $5^{\circ}\text{N}\text{--}10^{\circ}\text{N}$ within the upper core of the DWBC. The same order of magnitude is inferred from SOFAR float trajectories (velocities higher than 50 cm s^{-1} at 1800 m) in the DWBC (Richardson and Schmitz, 1993). Johns et al. (1993) discuss a very high variability at the 1600 m level from a current meter mooring at 8°N , 52°W from September 1987 to September 1988 (maximal southward velocity around 20 cm s^{-1}). Schott et al. (1993) describe near the equator at 44°W , at 1745 m depth, from September 1990 to September 1991, a well established mean southward current (maximal southward velocity reaching 50 cm s^{-1}).

Away from the DWBC, where waters are older (Fig. 9), there is no more bias due to the constancy of the F-11/F-12 ratio after 1975. But important dilution, self-mixing and recirculation still result in an over-estimate of the “apparent” age.

We have used three different methods in order to evaluate an “apparent” velocity along the equator. This “apparent” velocity is representative of the propagation rate of surface condition information through the system but not really to an advection speed:

- (1) We obtain a mean “apparent” velocity equal to 1.5 cm s^{-1} by dividing the 3300 km distance between 35°W and 4°W by the time lag resulting from the difference between the mean “apparent” ages at $3^{\circ}50\text{W}$ (26 years) and 35°W (19 years).
- (2) From the $3^{\circ}50\text{W}$ section alone (where the penetration of the CFM tongue occurs in a completely *freon*-free environment), the zonal “apparent” velocity deduced from the F-11/F-12 age method (assuming a 14,000 km distance from the Labrador Sea to the eastern equatorial Atlantic) is the same order of magnitude, around 1.9 cm s^{-1} .

Fig. 9. “Apparent age” distributions during CITHER 1 (contours in years): (a) northern section (WOCE A6) at $7^{\circ}30\text{N}$; (b) southern section (WOCE A7) at $4^{\circ}30\text{S}$; (c) meridional western section at 35°W ; (d) meridional eastern section at $3^{\circ}50\text{W}$. Shaded areas correspond to apparent age less than 25 years.





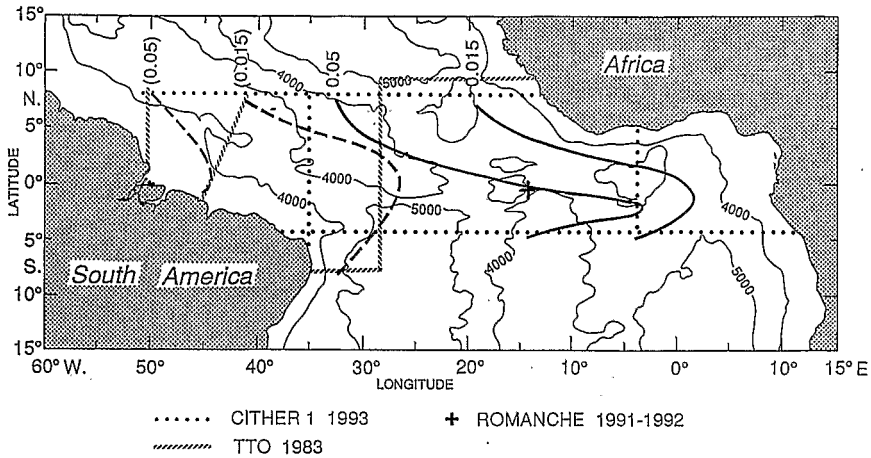


Fig. 10. TTO-CITHER 1 F-11 distributions comparison (0.015 and $0.05 \text{ pmol kg}^{-1}$ isolines). The 0.015 and 0.05 isolines relative to the 1983 data set (broken lines) are indicated in parenthesis. Superimposed is the 4000 m isobath at the location of the mid-Atlantic ridge. The plotted CFM contours are based, for each station, on the extreme values in the $1600\text{--}1800 \text{ m}$ layer.

- (3) We report in Fig. 10 the schematic horizontal distribution of the $0.015 \text{ pmol kg}^{-1}$ and $0.05 \text{ pmol kg}^{-1}$ isolines in the tropical area based on an interpolation between the four F-11 sections sampled during CITHER 1 at the UNADW level (1600 m). A complementary data set has been used at the equator around 15°W coming from the ROMANCHE cruises (Messias et al., 1998).

Drawing of the isolines was by hand, following a subjective interpolation, so their shapes must be considered with caution, taking into account the lack of data between the sampled sections. For comparison, the TTO 1983 and CITHER 1 F-11 distributions have been superimposed. Despite the very coarse resolution of this scheme, the eastward progression of the transient tracer is clearly seen between 1983 and 1993. We deduce a mean zonal “apparent” velocity of 1.4 cm s^{-1} inferred from the 4440 km eastward displacement (from $43^\circ 50' \text{ W}$ to $3^\circ 50' \text{ W}$), over 10 years, of the $0.05 \text{ pmol kg}^{-1}$ isoline (contours well above the analytical threshold for both cruises).

The similarity of the three speed estimates shows that, ultimately, these numbers reflect an overall integral aspect of the tracer distribution (Doney and Jenkins, 1994). Moreover, this evaluation is very close to that of Weiss et al. (1985) using SAVE data (around 1.4 cm s^{-1}). The “apparent” velocity can be seen as an integrated mean flow rate, including dilution processes and spatial and temporal variations, similar to a “spreading rate”.

Direct velocity measurements along the equator are slower than within the DWBC. Absolute velocities inferred from drifting floats at 1800 m depth along the equator (Richardson and Schmitz, 1993) give a mean eastward velocity around 4.1 cm s^{-1} in 1989 and a mean westward value of about -4.6 cm s^{-1} for the first 8 months of 1990 (inside the box $20\text{--}40^\circ\text{W}$, $2^\circ\text{5N}\text{--}2^\circ\text{5S}$). The few direct estimates inferred from current

meter measurements give maximal eastward velocities of about 10 cm s^{-1} (Ponte et al., 1990).

Due to the great current variability resulting from the non-permanent and reversing properties of the equatorial flow, there is an important discrepancy between maximal measured values (maximum of 10 cm s^{-1} , either eastward or westward) and the eastward mean velocity values (less than 1 cm s^{-1}). Richardson and Schmitz (1993) argue that “the equatorial currents act as a temporary reservoir for DWBC water, storing it in eastward flow and releasing it in westward flow”. Modeling results reported by Kawase et al. (1992) or Böning and Schott (1993) only suggest the existence of a mean, weak, eastward current along the equator.

5. Conclusion

The first pieces of information inferred from the CFM data set of the trans-Atlantic equatorial CITHER 1 cruise are particularly important to the NADW behavior in the meridional overturning circulation.

The presence of F-11 and F-12 signals in the eastern basin confirms the eastward bifurcation at the equator assumed by Weiss et al. (1985), particularly at the UNADW level. Eastward drifting buoy trajectories (Richardson and Schmitz, 1993) agree with the *freon* core observed south of the equator at 35°W . Direct measurements at 15°W (RFZ) show that the zonal currents at the 1700 m level are highly variable (Mercier, pers. comm.) with a weak mean eastward value, of the same order of magnitude as that evaluated from tracers ($<1 \text{ cm/s}$). At the LNADW level, the permanent eastward velocity ($>10 \text{ cm/s}$) measured in the bottom of the RFZ (Mercier, pers. comm.) corresponds to the high *freon* concentration measured in the fracture zone (Messias et al., 1998). The low *freon* concentration (close to the detection limit) observed at 4°W is due to cascading and intense mixing after crossing the sills of the RFZ.

Heterogeneous structures are observed at the UNADW and LNADW levels, which correspond to the *freon* cores of the direct DWBC and of the Guiana gyre as described in the circulation patterns of F&H93 and F&a.94. Additional information relates to:

- the width of the recirculating branch,
- the existence, at the UNADW level, of a permanent offshore southeastward flow, on the western flank of the MAR
- the recirculation gyre, which seems to occur also at the MNADW level.

The meridional distribution at 35°W shows a dominant bifurcated *freon* core associated with an eastward flow, shifted $2\text{--}3^\circ\text{S}$ south of the equator. Other alternate high and low CFM structures are observed in the depth range 1500–1900 m. This is in agreement with the theoretical study of deep equatorial jets (Hua et al., 1997), where thin zonal currents, alternately westward and eastward, are generated south and north of the equator (over a few tens of meters deep or a few degrees in longitude wide).

The “apparent” age distribution reflects the *freon* distributions: it illustrates the mean spreading rate distribution of the transient tracer all over the tropical Atlantic,

which is the relevant quantity in assessing the oceanic uptake of anthropogenic compounds such as CO₂.

Tracer data obtained through WOCE sections are expected to validate high resolution general circulation models, including topography, in order to approach realistic mean zonal and meridional deep transports. CITHER 1 F-11 data have provided details to the F&H93 and F&al.94 circulation patterns. The resulting global mass and heat interhemispheric exchanges should be fundamental in climate study.

The F-11 distribution obtained during the CITHER 1 cruise constitutes the snapshot of the deep tropical Atlantic circulation in the 1993 boreal winter. It shall be of great interest in the study of the DWBC temporal variability study, particularly over the half decade when tracer cruises were performed from 1990 (Meteor cruises Me14, Me16, Me22, Me27; Rhein et al., 1995) to 1996 (WOCE Etambot cruises).

Acknowledgements

The authors specially thank C. Oudot, chief of the project, and A. Morlière and C. Colin, chief scientists of the two legs. The captains and all the crew of the R.V. *Atalante* made possible the CFM measurements under very good conditions on board. We thank D. Nowicki and D. Corre for their help during data processing. We are particularly grateful to R. Fine, G. Reverdin, Y. Gouriou, M. Fieux, C. McNeil and R. Molcard for their helpful comments. The detailed comments of anonymous reviewers considerably helped the revision of the manuscript. This work was supported by ORSTOM (Institut Français de Recherche Scientifique pour le Développement en Coopération) and IFREMER (Institut Français de Recherche pour l'Exploitation de la MER). The program was part of the PNEDC (Programme National d'Etude de la Dynamique du Climat). This is a contribution to WOCE.

References

- Arhan, M., Mercier, H., Bourlès, B., Gouriou, Y., 1998. Hydrographic sections across the Atlantic at 7°30N and 4°30S. *Deep Sea Research I* 45, 829–872.
- Andrié, C., Ternon, J.F., 1994. Mesures des chorofluorométhane in: Campagne CITHER 1. Recueil de données CTDO2, vol. 3/4, Traceurs géochimiques (1), Documents Scientifiques du Centre ORSTOM de Cayenne, No. O.P. 15, pp. 67–77.
- Böning, C., Schott, F., 1993. Deep currents and the eastward salinity tongue in the equatorial Atlantic: results from an eddy-resolving, primitive equation model. *Journal of Geophysical Research* 98, 6991–6999.
- Bub, F.L., Brown, W.S., 1996. Intermediate layer water masses in the western tropical Atlantic Ocean. *Journal of Geophysical Research* 101, 11903–11922.
- Bullister, J.L., Weiss, R.F., 1988. Determination of CCl₃F and CCl₂F₂ in seawater and air. *Deep Sea Research* 35, 839–853.
- Bullister, J.L., Menzia, F., Wisegarver, D.P., 1993. WOCE 1991 Chlorofluorocarbon Standard Intercomparison Report. NOAA Data Report ERL PMEL-45, Seattle, 66 pp.

- Colin, C., Bourlès, B., 1994. Western boundary currents and transports off French Guiana as inferred from Pegasus observations. *Oceanologica Acta* 17, 143–157.
- Colin, C., Reppin, J., Bourlès, B., 1994a. Mesures de courants avec le profileur Pegasus. In: Campagne CITHER 1. Recueil de données. Vol. 1/4; Mesures “en route”, Courantométrie ADCP et PEGASUS. Documents scientifiques No: O.P. 14, Centre ORSTOM de Cayenne, pp. 145–161.
- Colin, C., Bourlès, B., Chuchla, R., Dangu, F., 1994b. Western boundary current variability off French Guiana from moored current measurements. *Oceanologica Acta* 17, 345–354.
- Dickson, R.R., Gmitrowitz, E.M., Watson, A.L., 1990. Deep. water renewal in the north Atlantic. *Nature* 344, 848–850.
- Dickson, R.R., Brown J., 1994. The production of North Atlantic Deep Water: Sources, rates and pathways. *Journal of Geophysical Research* 99, 12319–12341.
- Doney, S.C., Bullister, J.L., 1992. A chlorofluorocarbon section in the eastern North Atlantic. *Deep Sea Research* 39, 1857–1883.
- Doney, S.C., Jenkins, W.J., 1994. Ventilation of the deep western boundary current and abyssal western north Atlantic: estimates from tritium and ^3He distributions, *Journal of Physical Oceanography* 24, 638–659.
- Durrieu de Madron, X., Weatherly, G., 1994. Circulation, transport and bottom boundary layers of the deep currents in the Brazil basin. *Journal of Marine Research* 52, 583–638.
- Fine, R.A., Molinari, R.L., 1988. A continuous deep western boundary current between Abaco (26, 5°N) and Barbados (13°N). *Deep Sea Research* 35, 1441–1450.
- Fischer, J., Schott, F.A., 1997. Seasonal transport variability of the Deep Western Boundary Current in the equatorial Atlantic. *J. Geophys. Res.* 102, C13, 27751–27769.
- Friedrichs, M.A.M., Hall, M.M., 1993. Deep circulation in the tropical North Atlantic. *Journal of Marine Research* 51, 697–736.
- Friedrichs, M.A.M., McCartney, M.S., Hall, M.M., 1994. Hemispheric asymmetry of deep water transport modes in the western Atlantic. *Journal of Geophysical Research* 99, 25165–25179.
- Groupe CITHER 1, 1994a. Campagne CITHER-1. Recueil de données. Vol. 1/4: Mesures “en route”, Courantométrie ADCP et PEGASUS. Documents scientifiques No: O.P. 14, Centre ORSTOM de Cayenne, 161 pp.
- Groupe CITHER 1, 1994b. Campagne CITHER-1. Recueil de données. Vol. 2/4: CTD-O2. Rapport interne LPO 94-04, Laboratoire de Physique des Océans, Brest.
- Groupe CITHER 1, 1994c. Campagne CITHER-1. Recueil de données. Vol. 3/4: Traceurs géochimiques (1). Documents scientifiques N°OP 15, Centre ORSTOM de Cayenne, 525 pp.
- Hall, M.M., McCartney, M., Whitehead, J.A., 1997. Antarctic Bottom Water flux in the equatorial western Atlantic. *Journal of Physical Oceanography* 27, 1903–1920.
- Hua, B.L., Moore, D.W., Le Gentil, S., 1997. Inertial nonlinear equilibration of equatorial flows. *J. Fluids Mechanics* 331, 345–371.
- Johns, W.E., Fratantoni, D.M., Zantopp, R.J., 1993. Deep western boundary current variability off northeastern Brazil. *Deep Sea Research* 40, 293–310.
- Kawase, M. (1987) Establishment of deep ocean circulation driven by deep-water production, *Journal of Physical Oceanography* 17, 2294–2317.
- Kawase, M., 1993. Topographic effects on the bottom water circulation of the western tropical north Atlantic ocean. *Deep Sea Research* 40, 1259–1283.
- Kawase, M., Rothstein, L.M., Spriinger, S.R., 1992. Encounter of a deep western boundary current with the equator: a numerical spin-up experiment. *Journal of Geophysical Research* 97, 5447–5463.

- Kawase, M., Sarmiento, J.L., 1986. Circulation and nutrients in middepth Atlantic waters. *Journal of Geophysical Research* 91, 9749–9770.
- Lazier, J.R.N., 1973. The renewal of Labrador Sea water. *Deep Sea Research* 20, 341–353.
- Lazier, J.R.N., 1988. Temperature and salinity changes in the deep Labrador Sea, 1962–1986. *Deep Sea Research* 35, 1247–1253.
- McCartney, M.S., 1993. Crossing of the equator by the Deep Western Boundary Current in the Western Atlantic Ocean. *Journal of Physical Oceanography* 23, 1953–1974.
- McCartney, M.S., Bennett, S.L., Woodgate-Jones, M.E., 1991. Eastward flow through the Mid-Atlantic Ridge at 11°N and its influence on the abyss of the eastern basin. *Journal of Physical Oceanography* 21, 1089–1121.
- McCartney, M.S., Curry, R.A., 1993. Transequatorial flow of Antarctic bottom water in the western Atlantic ocean: abyssal geostrophy at the equator. *Journal of Physical Oceanography* 23, 1264–1276.
- Mercier, H., Speer, K.G., Honnorez, J., 1994. Flow pathways of bottom water through the Romanche and Chain Fracture Zones. *Deep Sea Research* 41, 1457–1477.
- Mercier, H., Billant, A., Brancellec, P., Andrié, C., Messias, M.J., Gouriou, Y., Laguadec, C., 1995. Campagne Romanche 2 – Données de la sonde CTDO₂, Mesures de Salinité, d'Oxygène dissous et des Chlorofluorométhane, Courantométrie Acoustique Doppler. Rapport Interne LOP 95-02, Brest, 147 pp.
- Mercier, H., Morin, P., 1997. Hydrography of the Romanche and Chain Fracture Zones. *Journal of Geophysical Research* 102, 10373–10389.
- Messias, M.J., Andrié, C., Memery, L., Mercier, H., 1998. Tracing the North Atlantic Deep Water through the Romanche and Chain fracture zones using chlorofluoromethanes. *Deep Sea Research*, in press.
- Molinari, R.L., Fine, R.A., Johns, E., 1992. The Deep Western Boundary Current in the tropical North Atlantic Ocean. *Deep Sea Research* 39, 1967–1984.
- Oudot, C., Morin, P., Baurand, F., Wafar, M., Le Corre, P., 1998. Northern and southern water masses in the equatorial Atlantic sector: distribution of nutrients on the WOCF A6 and A7 lines. *Deep Sea Research I* 45, 873–902.
- Pickart, R.S., Hogg, N.G., Smethie, W.M. Jr., 1989. Determining the strength of the deep western boundary current using the chlorofluoromethane ratio. *Journal of Physical Oceanography* 19, 940–951.
- Pickart, R.S., 1992. Water mass components of the North Atlantic deep western boundary current. *Deep Sea Research* 39, 1553–1572.
- Pickart, R.S., Hogg, N.G., 1989. A tracer study of the deep Gulf Stream cyclonic recirculation. *Deep Sea Research* 36, 935–956.
- Pickart, R.S., Smethie, W.M. Jr., 1993. How does the deep western boundary current cross the Gulf Stream; *Journal of Physical Oceanography* 23, 2602–2616.
- Polzin, K.L., Speer, K.G., Toole, J.M., Schmitt, R.W., 1996. Intense mixing of Antarctic Bottom Water in the equatorial Atlantic ocean. *Nature* 380, 54–57.
- Ponte, R.M., Luyten, J., Richardson, P.L., 1990. Equatorial deep jets in the Atlantic ocean. *Deep Sea Research* 37, 711–713.
- Reid, J.L., 1994. On the total geostrophic circulation of the North Atlantic ocean: flow patterns, tracers, and transports. *Progress in Oceanography* 33, 1–92.
- Rhein, M., 1994. The Deep Western Boundary Current: tracers and velocities. *Deep Sea Research* 41, 263–281.
- Rhein, M., Stramma, L., Send, U., 1995. The Atlantic Deep Western Boundary Current: water masses and transports near the equator. *Journal of Geophysical Research* 100, 2441–2457.

- Richardson, P., Zemanovic, M.E., Wooding, C.M., Schmitz, W.J. Jr., 1994. SOFAR float trajectories in the Tropical Atlantic 1989–1992. Technical Report WHOI-94-93, Woods Hole Oceanographic Institution, 185 pp.
- Richardson, P.L., Schmitz, W.J. Jr., 1993. Deep cross-equatorial flow in the Atlantic measured with SOFAR floats. *Journal of Geophysical Research* 98, 8371–8387.
- Schott, F., Fisher, J., Reppin, J., Send, U., 1993. On mean and seasonal currents and transports at the western boundary of the equatorial Atlantic. *Journal of Geophysical Research* 98, 14353–14368.
- Smethie, Jr. W. 1993. Tracing the thermohaline circulation in the western North Atlantic using chlorofluorocarbons. *Progress in Oceanography* 31, 51–99.
- Speer, K.G., 1993. The deep silica tongue in the north Atlantic. *Deep Sea Research* 40, 925–936.
- Speer, K.G., McCartney, M.S., 1991. Tracing lower north Atlantic deep water across the equator. *Journal of Geophysical Research* 96, 20443–20448.
- Talley, L.D., Johnson, G.C., 1994. Deep, zonal subequatorial currents. *Science* 263, 1125–1128.
- Talley, L.D., McCartney, M.S., 1982. Distribution and circulation of Labrador Sea water. *Journal of Physical Oceanography* 12, 1189–1205.
- Tsuchiya, M., Talley, L.D., McCartney, M.S., 1992. An eastern Atlantic section from Iceland southward across the equator. *Deep Sea Research* 39, 1885–1917.
- Tsuchiya, M., Talley, L.D., McCartney, M.S., 1994. Water-mass distributions in the western South Atlantic; a section from South Georgia Island (54S) northward across the equator. *Journal of Marine Research* 52, 55–81.
- Wallace, D.W.R., Lazier, J.R.N., 1988. Anthropogenic chlorofluoromethanes in newly formed Labrador sea water. *Nature* 332, 61–63.
- Warner, M.J., Weiss, R.F., 1985. Solubilities of chlorofluorocarbons 11 and 12 in water and seawater. *Deep Sea Research* 32, 1485–1497.
- Weiss, R.F., Bullister, J.L., Gammon, R.H., Warner, M.J., 1985. Atmospheric chlorofluoromethanes in the deep equatorial Atlantic. *Nature* 314, 608–610.
- Weisse, R., Mikolajewicz, U., Maier-Reimer, E., 1994. Decadal variability of the North Atlantic in an ocean general circulation model. *Journal of Geophysical Research* 99, 12411–12421.